Wave Initiation through Spatiotemporally Controllable Perturbations

J. Wolff, A. G. Papathanasiou, H. H. Rotermund,* and G. Ertl
Fritz-Haber-Institut der Max-Planck-Gesellschaft, Faradayweg 4-6, 14195 Berlin, Germany

M. A. Katsoulakis
Department of Mathematics and Statistics, University of Massachusetts, Amherst, Massachusetts, 01003

X. Li and I. G. Kevrekidis
Department of Chemical Engineering, Princeton University, Princeton, New Jersey, 08544
(Received 13 November 2002; published 9 April 2003)

We study the initiation of pulses and fronts in a two-dimensional catalytic reaction-diffusion system: CO oxidation on Pt(110). Using a computer-controlled mobile focused laser beam, we impart various patterns (in space and time) of localized temperature "kicks" to the surface. We explore, and also rationalize through modeling, the cooperativity of such individually subcritical perturbations in both the excitable and the bistable regime.

DOI: 10.1103/PhysRevLett.90.148301 PACS numbers: 82.45.Jn, 05.45.–a, 82.40.Bj, 82.40.Np

Introduction.—The interaction of reaction and transport is known to lead to spontaneous pattern formation in many physicochemical systems [1,2]. As the essential features of nonequilibrium spatiotemporal dynamics in uniform media are gradually understood, the "robustness" of the basic phenomenology to noise (perturbations in the medium properties, spontaneous fluctuations, variations in the operating conditions) become the focus of current research [3–9]. Periodic operation [10–13], local [14–16] and global [17,18] feedback, as well as the dynamics on composite catalysts [19,20] are examples of such studies under nonsteady/nonuniform conditions. The effects of spontaneous fluctuations on system dynamics become increasingly important in microscopic and nanoscopic systems. A strong drive for developing mathematical methods for the analysis of stochastic fluctuations originates thus in modern materials science and also in cellular biology.

The low-pressure oxidation of CO on Pt single crystal surfaces has emerged over the last decade as a paradigm for the study of spatiotemporal dynamics [21–23]. We recently constructed an "addressable catalyst," using computer-controlled galvanometer mirrors to move a focused laser beam ("pixel" size $\sim 50\ \mu$m) at will across a catalyst surface [24]. The beam results in a localized temperature heterogeneity, which, through the Arrhenius temperature dependence of kinetic processes, perturbs the (relatively slow) spatiotemporal system dynamics.

Concentration pulses and fronts constitute the basic building blocks of catalytic spatiotemporal dynamics. The notions of excitability (associated with the generation and spatial propagation of pulses) and bistability (correspondingly associated with fronts), constitute a cornerstone of mathematical pattern formation theory. Such patterns are typically generated from a uniform state through a single, localized in space and time, perturbation—a critical "kick" (e.g., see the wonderful original reference [25]). Here, we study the simplest cases of "spatiotemporally resolved" critical kicks in both the excitable and the bistable case. Using our mobile laser beam, we deliver different combinations of individually subcritical perturbations, and explore their cooperative behavior across space and time. In effect, these combinations constitute the simplest realizations of colored "designer noise."

The experimental capability of implementing arbitrary spatiotemporal forcings provides a platform for exploring stochastic dynamics for an active, pattern forming medium. In particular such experiments can be used to test and validate theoretical predictions for optimal switching paths and rare event rates obtained through large deviation techniques and dynamic programming [26,27].

Experimental.—Experiments were performed in an ultrahigh-vacuum (UHV) chamber, equipped with low-energy electron diffraction (LEED), Ar-ion sputtering, and catalyst sample heating (from the back side) via a halogen lamp. The 10 mm diameter sample was prepared by repeated cycles of Ar^+ sputtering and O_2 treatment at 570 K, and subsequent annealing to 1000 K. Gas supplies for CO and O_2, and pressure gauges, allow for controlled dosing of the reactants. Adsorbate concentration patterns on the surface of the sample are imaged using ellipsomicroscopy for surface imaging (EMSI) [28]. The light of another Ar-ion laser is focused onto a spot of about 50 μm diameter on the surface causing a local temperature increase of up to 10 K. Using computer-controlled galvanometer mirrors, the focused laser beam can be positioned in 1 ms with a spatial precision of 5 μm anywhere within the viewing field (1.5×1.3 mm).

During the experiment the laser was kept permanently on the sample, at the edge of the viewing field, in order to

ensure a constant background temperature. It was moved to the point of interest for a time interval t_1, and then, depending on the type of experiment, it was moved directly to a second spot for a time interval t_2, or back to its "waiting" position for a delay time t_d; from there it visited either the same first spot, or a second one, for a time interval t_2. For each series of trials below, the CO partial pressure was kept constant; 10 s before the first laser movement, oxygen partial pressure was raised suddenly to its default value of 3×10^{-4} mbar. The critical time for single-visit ignition (t_{crit}) as well as for combinations of two (individually subcritical) laser shots (t_1 and t_2) were thus recorded, and the results scaled with the appropriate t_{crit}. The distance (in space and time) of these combined subcritical shots, along with the laser intensity, parametrize our family of structured critical perturbations.

Modeling.—The currently accepted mechanism of low-pressure CO oxidation on Pt(110) is described through a three-species reaction-diffusion type model. This Krischer-Eiswirth-Ertl (KEE) model [29] embodies adsorption and desorption of CO and O_2, CO surface diffusion, reaction to form CO_2 as well as surface conversion between a reconstructed missing row 1×2 surface and its 1×1 lifting, depending on the CO coverage:

$$\frac{\partial u}{\partial t} = k_u s_u p_{\mathrm{CO}} \left[1 - \left(\frac{u}{u_s}\right)^3\right] - k_2 u - k_3 u v + \nabla \cdot (D \nabla u),$$

$$\frac{\partial v}{\partial t} = k_v p_{O_2} [w s_{v1} + s_{v2}(1 - w)] \left(1 - \frac{u}{u_s} - \frac{v}{v_s}\right)^2 - k_3 u v,$$

$$\frac{\partial w}{\partial t} = k_5 [f(u) - w]. \qquad (1)$$

Here u and v denote the surface coverage of CO and O, respectively; w is the fraction of the surface area in the 1×1 phase; $f(u)$ is an experimental fit to the rate of change of the surface structure and takes the following form for a Pt(110) surface:

$$f(u) = \begin{cases} 0 & u \le 0.2, \\ -\frac{u^3 - 1.05u^2 + 0.3u - 0.026}{0.0135} & 0.2 < u < 0.5, \\ 1 & u \ge 0.5. \end{cases}$$

In this model, the control parameters are the partial pressures of CO and O_2, and the crystal temperature field T, which enters the rate constants k_2, k_3, and k_5 through Arrhenius activation: $k_i = (k^0)_i \exp(-E_i/RT)$. Here, k_2, k_3, and k_5 represent the rate constants for the CO desorption, surface reaction, and reconstruction, respectively. The preexponential factors and activation energies we used in all our simulations are the ones listed in Table II of the original reference [29]. The spatially localized, single-humped steady temperature profile $\Phi(\mathbf{x}-\mathbf{x_0})$ with maximum temperature rise ΔT resulting from focusing the laser spot at a point $\mathbf{x_0}$ is dictated by the heat balance on the crystal surface. This balance involves heat conduction and radiation as well as heating from the laser; the heat generated from the reaction is comparatively negligible at these low pressures. Since the diffusivity of heat ($\sim 10^{-1}$ cm^2/s) is much larger than that of the adsorbed carbon monoxide ($\sim 10^{-7}$ cm^2/s) under typical experimental conditions, the temperature field rise time (milliseconds) is fast compared to reaction wave propagation (seconds). We thus assume for a first approximation that a steady temperature field $\Phi(\mathbf{x}-\mathbf{x_0})$ is instantaneously switched "on" and "off" by moving the laser spot to and from the point of interest $\mathbf{x_0}$. For a careful discussion of temperature field dynamics for both thick and thin crystals, see Ref. [30]. In our qualitative modeling, single spot simulations were radially symmetric, while two-spot simulations were one-dimensional in space; the same temperature profile was used in both. Similar qualitative results were obtained by using Gaussian temperature profiles.

Results.—Figure 1(a) shows the boundary (in two parameter space) of "single-spot excitability" as a function of p_{CO} at two distinct base crystal temperatures and $p_{O_2} = 3 \times 10^{-4}$ mbar. Single spot excitability refers to the generation of reactive pulses as a result of heating locally at one point in space continuously over a single time interval. The curves show the duration necessary for

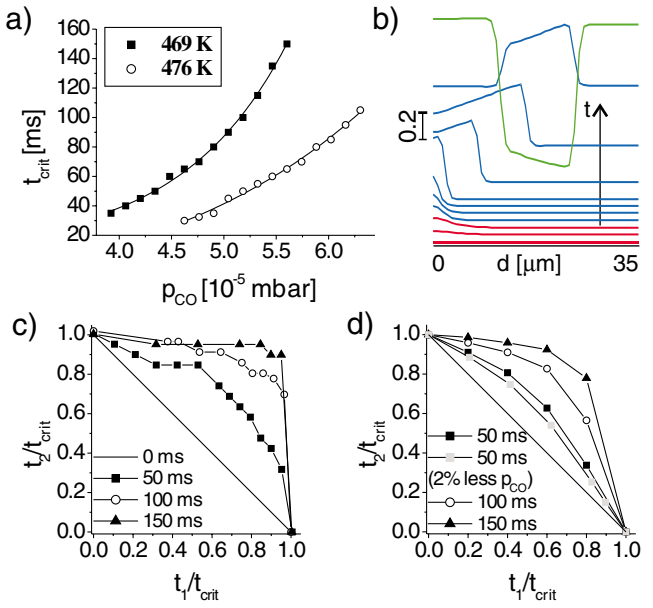

FIG. 1 (color). (a) Experimental t_{crit} for two sample temperatures, laser power 2 W, $p_{O_2} = 3.0 \times 10^{-4}$ mbar; the experimental error is estimated to be about ± 3 ms. (b) Computed v profiles showing the ignition. Red: during heating; blue: after heating; green: final u profile. $p_{\mathrm{CO}} = 4.95 \times 10^{-5}$ mbar, $p_{O_2} = 1.33 \times 10^{-4}$ mbar, $T = 535.5$ K, $\Delta T = 3.5$ K. (c) Experimental conditions: $p_{\mathrm{CO}} = 5.3 \times 10^{-5}$ mbar, $p_{O_2} = 3 \times 10^{-4}$ mbar, $T = 473$ K, laser power 2 W. (d) Computational parameters: $p_{\mathrm{CO}} = 5.0 \times 10^{-5}$ mbar, $p_{O_2} = 1.33 \times 10^{-4}$ mbar, $T = 535.5$ K, $\Delta T = 3.5$ K.

a 2 W laser shot (Pt reflectivity estimated at 70%) to ignite a self-sustaining concentration pulse. Figure 1(b) shows a succession of computed radial profiles of the (axisymmetric) O coverage fields for a "critical" shot; the included final CO coverage profile demonstrates CO depletion under the progressing oxygen pulse.

Figure 1(c) quantifies the memory effect of a subcritical shot. At these conditions and laser power a single shot becomes critical (initiates a pulse) after 80 ms. During a "double shot" excitability experiment the laser pixel heats a catalyst location for a subcritical duration, is removed for a period of time, and then visits the same location again. The time required for this second shot to ignite a pulse is plotted versus the initial shot duration (both normalized by the critical single-shot duration). The closer the points lie to the diagonal, the better the memory of the first shot is retained; on the other hand, when the abscissa approaches one, this memory is completely lost. Figure 1(d) is a computational analog of Fig. 1(c); we have included for comparison a single curve obtained at a different p_{CO}. Decreasing p_{CO} appears to strengthen the memory of the first shot; this can be rationalized by the slower readsorption of CO, delaying "healing" of the first shot.

Figure 2(a) illustrates the cooperative effect between a subcritical shot at one location and an immediate subsequent shot at a nearby location. Here again the duration of each shot is normalized by the single critical shot duration; separate curves are obtained for different separations of the two shot centers in space. Cooperativity visibly extends under these conditions for distances of $\sim 25\ \mu$m. Figure 2(b) shows a succession of computed radial profiles of the O coverage fields for a double shot. Notice how, in this case, heating at a distance of 50 μm from the original shot assists ignition at the primary shot location. For weak primary shots, the ignition will preferentially take place at the secondary shot location instead; we even observed once experimentally the "transition case" where both points "fired" simultaneously. It is interesting that taking the spatial step along different directions has a clear effect on the critical ignition times [Fig. 2(c)], which is at least in part caused by anisotropic surface diffusion.

The effect of a time delay between a first shot at one location and a second shot at a different location in space is illustrated in Fig. 2(d). Here, the distance between the shot locations is fixed and the effect of delay between the two shots is reported.

In the bistable regime laser shots initiate fronts rather than pulses. Since a bistable regime lies within the parameter range accessible to our experiment, we also examined cooperativity of subcritical shots in initiating reacting *fronts*. Experimentally, the fronts are initiated in the form of elliptical oxygen islands, and proceed to expand and "switch" the surface from the CO-poisoned, unreactive state to the reactive one. Figure 3(a) shows a computational snapshot sequence along such a one-dimensional computational transient. The cooperativity of separated in time subcritical shots at the same spatial location is quantified in Fig. 3(b) (experimentally) and Fig. 3(c) (computationally).

So far we have studied shot patterns in space and time that can be realized through a single laser beam. Figure 4(a) explores computationally the cooperativity of

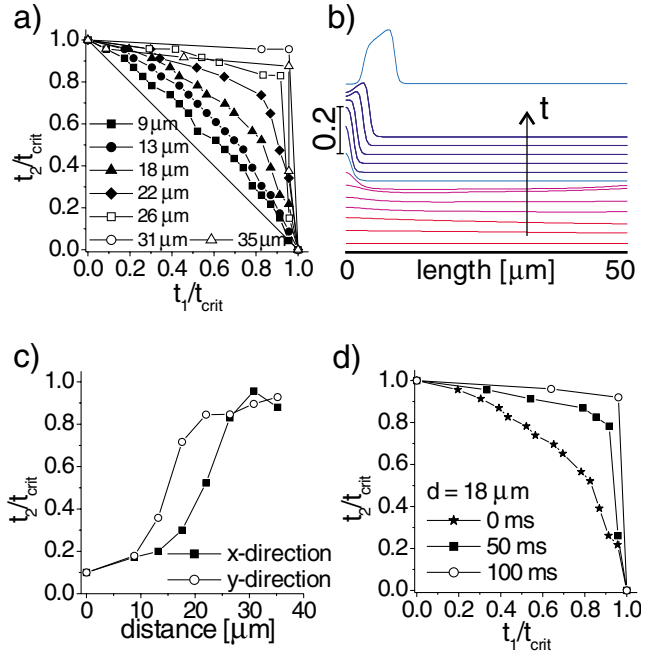

FIG. 2 (color). (a) Experimental conditions: $p_{CO} = 4.9 \times 10^{-5}$ mbar, $p_{O_2} = 3 \times 10^{-4}$ mbar, $T = 467$ K, laser power 2 W. (b) Computed υ profiles: first heating (red), second heating (violet), after heating (blue). Heat point $x = 0$ for 0.8 t_{crit}, then heat $x = 50$ for 0.77 t_{crit}. It fires at $x = 0$. $p_{CO} = 4.95 \times 10^{-5}$ mbar, $p_{O_2} = 1.33 \times 10^{-4}$ mbar, $T = 535.5$ K, $\Delta T = 3.5$ K. (c),(d) Experimental conditions as in (a).

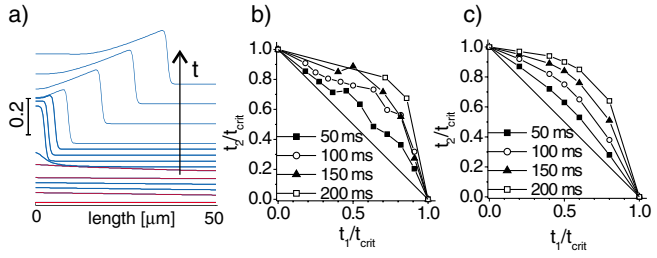

FIG. 3 (color). (a) Computed υ profiles: red: heating, blue: not heating. $p_{CO} = 4.8 \times 10^{-5}$ mbar, $p_{O_2} = 2.0 \times 10^{-4}$ mbar, $T = 535.5$ K, $\Delta T = 3.5$ K. Heat $x = 0$ for 0.6 t_{crit}, then pause for 0.7 t_{crit}, then heat for another 0.6 t_{crit}. (b) Experimental conditions: $p_{CO} = 2.1 \times 10^{-5}$ mbar, $p_{O_2} = 3 \times 10^{-4}$ mbar, $T = 429$ K, laser power 3 W. (c) computational conditions: $p_{CO} = 4.8 \times 10^{-5}$ mbar, $p_{O_2} = 2.0 \times 10^{-4}$ mbar, $T = 535.5$ K, $\Delta T = 3.5$ K (the laser power is about 0.2 W).

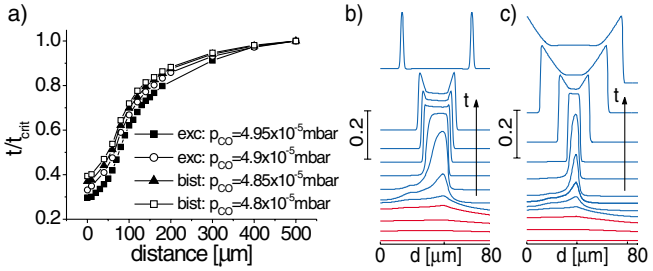

FIG. 4 (color). (a) Computational parameters: $T = 535.5$ K, $p_{O_2} = 2.0 \times 10^{-4}$ mbar, $\Delta T = 3.5$ K. (b),(c) Transient profiles for v. Only half of the domain is shown. The two spots are at $x = -45$ and $x = 45$, respectively. $T = 535.5$ K, $p_{O_2} = 2.0 \times 10^{-4}$ mbar, $\Delta T = 3.5$ K. p_{CO} is 4.95×10^{-5} mbar in (b) and 4.8×10^{-5} mbar in (c).

two shots, separated in space but simultaneous in time. It is interesting to notice that, for both pulse (excitable) and front (bistable) nucleation, the least energy required for ignition occurs when the two beams effectively heat the same point. Alternatively, doubling the laser power requires less than half the energy to ignite a spot—this is because of the nonlinear (Arrhenius) temperature dependence of the kinetic rates. Figures 4(b) and 4(c) show transient ignitions of pulses (excitable) and fronts (bistable), respectively.

We have examined *deterministic* critical perturbations, capable of switching the surface from a spatially uniform, stable steady state X_1 to a different state X_2—either another uniform, stable steady state, or a traveling pulse state. Realizing that the set of "all possible deterministic perturbations" and the set of "all possible random perturbations" are, in effect, the same, it is interesting to consider the subset of *random* perturbations capable of switching the surface between two uniform states, or firing a pulse, using established methods (such as large deviation theory and the study of rare events) from the theory of stochastic PDEs (see [3,31] for a review). Based on the experimental ability to implement a rich variety of random colored noise processes, we expect this setup to provide an ideal vehicle for such studies. The spatiotemporal versions of excitability and bistability ("firing" and switching) examined here constitute the first step in this direction.

The support of NSF (MAK, XL, IGK), AFOSR and a Humboldt Prize (IGK) are gratefully acknowledged.

*Corresponding author.
Email address: rotermun@fhi-berlin.mpg.de

[1] Y.-J. Li, J. Oslonovitch, N. Mazouz, F. Plenge, K. Krischer, and G. Ertl, Science **291**, 2395 (2001).
[2] A. N. Zaikin and A. M. Zhabotinsky, Nature (London) **225**, 535 (1970).
[3] A. S. Mikhailov, Phys. Rep. **184**, 307 (1989).
[4] A. J. Irwin, S. J. Fraser, and R. Kapral, Phys. Rev. Lett. **64**, 2343 (1990).
[5] P. Jung and G. Mayer-Kress, Phys. Rev. Lett. **74**, 2130 (1995).
[6] K. Wiesenfeld and F. Moss, Nature (London) **373**, 33 (1995).
[7] J. M. G. Vilar and J. M. Rubí, Phys. Rev. Lett. **78**, 2886 (1997).
[8] S. Kádár, J. Wang, and K. Showalter, Nature (London) **391**, 770 (1998).
[9] H. Hempel, L. Schimansky-Geier, and J. García-Ojalvo, Phys. Rev. Lett. **82**, 3713 (1999).
[10] O. Steinbock, V. Zykov, and S. C. Müller, Nature (London) **366**, 322 (1993).
[11] V. Petrov, Q. Ouyang, and H. L. Swinney, Nature (London) **388**, 655 (1997).
[12] A. L. Lin, M. Bertram, K. Martinez, and H. L. Swinney, Phys. Rev. Lett. **84**, 4240 (2000).
[13] I. Sendiña-Nadal, E. Mihaliuk, J. Wang, V. Pérez-Muñuzuri, and K. Showalter, Phys. Rev. Lett. **86**, 1646 (2001).
[14] S. Grill, V. S. Zykov, and S. C. Müller, Phys. Rev. Lett. **75**, 3368 (1995).
[15] S. Sinha and N. Gupte, Phys. Rev. E **58**, R5221 (1998).
[16] T. Sakurai, E. Mihaliuk, F. Chirila, and K. Showalter, Science **296**, 2009 (2002).
[17] V. K. Vanag, L. Yang, M. Dolnik, A. M. Zhabotinsky, and I. R. Epstein, Nature (London) **406**, 389 (2000).
[18] M. Kim, M. Bertram, M. Pollmann, A. v. Oertzen, A. S. Mikhailov, H. H. Rotermund, and G. Ertl, Science **292**, 1357 (2001).
[19] N. Hartmann, M. Bär, K. Krischer, I. G. Kevrekidis, and R. Imbihl, Phys. Rev. Lett. **76**, 1384 (1996).
[20] M. Pollmann, H. H. Rotermund, G. Ertl, X. Li, and I. G. Kevrekidis, Phys. Rev. Lett. **86**, 6038 (2001).
[21] H. H. Rotermund, W. Engel, M. Kordesch, and G. Ertl, Nature (London) **343**, 355 (1990).
[22] M. D. Graham, I. G. Kevrekidis, K. Asakura, J. Lauterbach, K. Krischer, H. H. Rotermund, and G. Ertl, Science **264**, 80 (1994).
[23] K. C. Rose, B. Berton, R. Imbihl, W. Engel, and A. M. Bradshaw, Phys. Rev. Lett. **79**, 3427 (1997).
[24] J. Wolff, A. G. Papathanasiou, I. G. Kevrekidis, H. H. Rotermund, and G. Ertl, Science **294**, 134 (2001).
[25] N. Wiener and A. Rosenblueth, Arch. Inst. Cardiol. Mexico **16**, 205 (1946).
[26] M. I. Freidlin and A. D. Wentzell, *Random Perturbations of Dynamical Systems* (Springer, Berlin, 1998), 2nd ed.
[27] D. P. Bertsekas, *Dynamic Programming: Deterministic and Stochastic Models* (Prentice Hall, Englewood Cliffs, 1987).
[28] H. H. Rotermund, G. Haas, R. U. Franz, R. M. Tromp, and G. Ertl, Science **270**, 608 (1995).
[29] K. Krischer, M. Eiswirth, and G. Ertl, J. Chem. Phys. **96**, 9161 (1992).
[30] J. Cisternas, P. Holmes, I. G. Kevrekidis, and X. Li, J. Chem. Phys. **118**, 3312 (2003).
[31] A. S. Mikhailov and A. Y. Loskutov, *Foundations of Synergetics II: Chaos and Noise* (Springer, Berlin, 1996), 2nd ed.